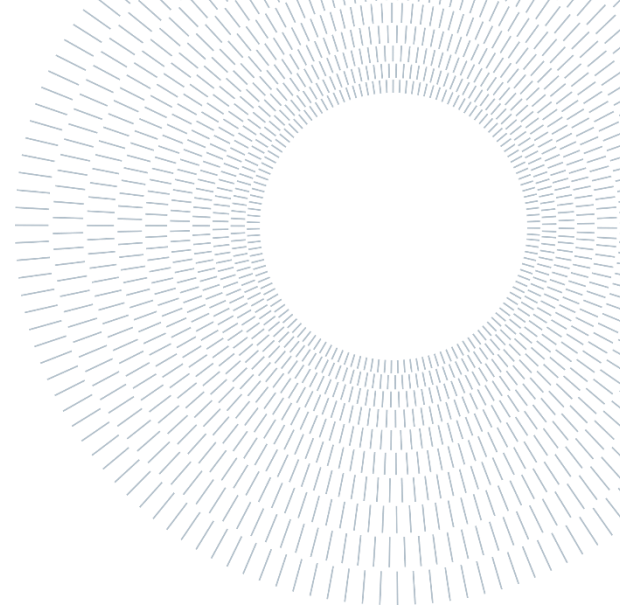




POLITECNICO
MILANO 1863

SCUOLA DI INGEGNERIA INDUSTRIALE
E DELL'INFORMAZIONE



EXECUTIVE SUMMARY OF THE THESIS

Study of the radiation field of the ALFA station at ELI Beamlines

TESI MAGISTRALE IN NUCLEAR ENGINEERING – INGEGNERIA NUCLEARE

Author: **Francesco BRAVIN**

Advisor: Marco CARESANA

Co-Advisor: Roberto VERSACI

Academic Year: 2023-2024

1. Introduction

Precise dosimetry is critical to ensure safety and optimize operational efficacy in laser-driven accelerator settings. This work investigates the secondary radiation field produced by a laser-driven electron accelerator, specifically focusing on the Allegra Laser For Acceleration (ALFA) experimental station at the Extremelight Infrastructure (ELI) Beamlines facility in the Czech Republic.

While dosimeters designed for operation in pulsed fields are commercially available, none are specifically tailored to function effectively under the challenging conditions existing in the vicinity of a laser-driven accelerator. The technological challenges include the ultra-short duration of the laser pulses, the mixed radiation field generated by the interaction of the primary beam with its surroundings, and the intense electromagnetic pulses resulting from the laser-plasma interaction [1].

This investigation is conducted through the analysis of dosimetric measurements collected by the three different dosimeters, supplemented by Monte Carlo simulations to support the underlying physical and technical considerations.

2. ELI Beamlines

The study has been carried out at the ELI Beamlines facility, which is part of the ELI-ERIC consortium, the largest international network of civilian laser-based user facilities.

ELI Beamlines is equipped with four primary high-peak-power femtosecond laser systems with high-energy and high-repetition-rate capabilities. These primary sources support a dozen experimental stations, which enable research in interaction of light with matter (plasma) at ultrahigh laser intensities.

This is of large importance for front-edge high-field physics, nuclear fusion, and laboratory astrophysics, and also for materials science, biology, chemistry, medicine and other

disciplines with strong multidisciplinary application potential.

3. Setup

3.1. ALFA station

The ALFA electron beam source employs laser wakefield acceleration technology to generate relativistic pulsed electron beams.

In this system the beam is produced by focusing of the laser beam (up to 32 mJ pulse energy and 15 - 20 fs pulse length range at 1 kHz) generated by L1-Allegria laser system into a gas target. The target kinetic energy of the electron beam is designed to be within the range of 1 to 100 MeV, which represents an unprecedented energy level for LWFA operating at a frequency of 1 kHz [2].

The setup of the ALFA station during the data taking campaign included a slit and a 0.1 T dipole magnet. A Lanex screen was also mounted at the viewport for spectroscopy purposes, along with a 160 mm diameter flange as viewport. A picture of the ALFA setup is shown in **Figure 1**, and a representation of the CAD drawing of the ALFA vacuum chamber is provided in **Figure 2**.

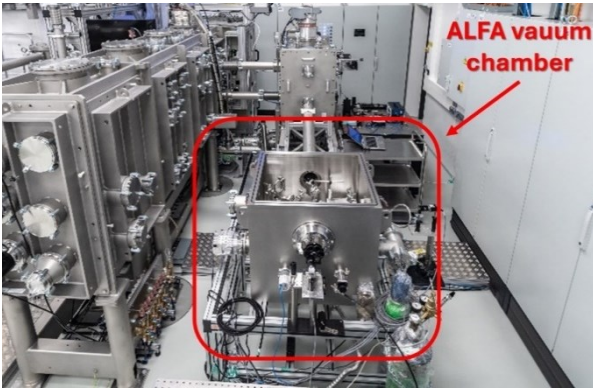


Figure 1: Image of a portion of the ALFA experimental hall. The ALFA vacuum chamber is highlighted within the red rectangle.

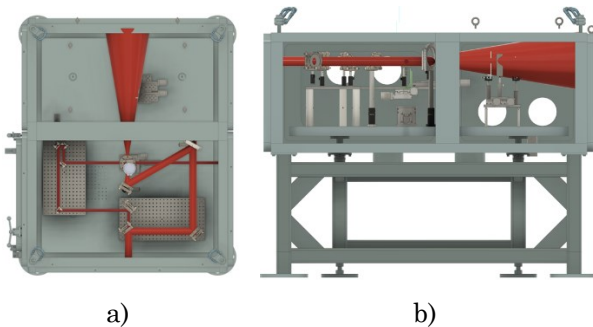


Figure 2: CAD drawing of the ALFA vacuum chamber and its components. Top (a) and side (b) view.

3.2. Dosimeters

The ALFA experimental station has been outfitted with three active dosimeters that can record both the dose rate ($\mu\text{Sv/h}$) and the total dose (μSv). The Lupin BF3-NP dosimeter measures the dose-rate delivered by the neutrons only, while the Nausicaa ICP-T-PF measures the dose-rate from gamma radiation. The LB6419 dosimeter, also known as Pandora, features two distinct and independent detection channels, enabling simultaneous measurement of both neutrons and gammas.

Consequently, the selection of these three dosimeters facilitates a side-by-side comparison of both types of radiation, thus enhancing the understanding of the radiation field, which is not known in advance. Additionally, a comparison of their results provides insight into their behavior in an ultra-short pulsed radiation field. **Table 1** summarizes the main characteristics of the three dosimeters.

	Lupin BF3-NP	Nausicaa ICP-T-PF	LB6419
Detection	Neutrons	Gamma part.	Gamma part. & Neutrons
Energy Range	0.025 eV – 10 GeV	30 keV – 10 MeV	N.A.
Sensitivity	0.6 cps/ $\mu\text{Sv/h}$	$2 \cdot 10^{-8}$ A/R/h	N.A.
Dose-Rate Range	10 nSv/h – 0.1 Sv/h	10 nSv/h – 0.1 Sv/h	N.A.

Table 1: Main features of the utilized dosimeters.

The detectors have been arranged on a table at an approximate height of 116 cm, positioned side by side. A beam dump, consisting of a 50 cm thick granite slab and a 10 cm thick lead slab, is also present to shield radiation from the corridor located behind it. The table supporting the detectors is situated 7 meters from the source and at an angle of approximately 30 degrees relative to the beam axis, adjacent to the beam dump, as schematically illustrated in **Figure 3**. A photograph of the detector is also presented in **Figure 4**. Furthermore, two additional Pandora detectors have been placed within the experimental hall to collect supplementary data: one located in the west corridor, directly behind the beam dump, and the other situated in the control room (refer to Figure 3).

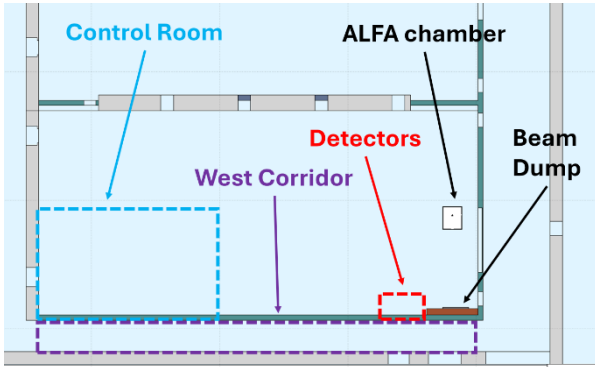


Figure 3: Top view of the FLUKA geometry model of the ALFA experimental hall. Dashed colored boxes delineate significant areas of the model.

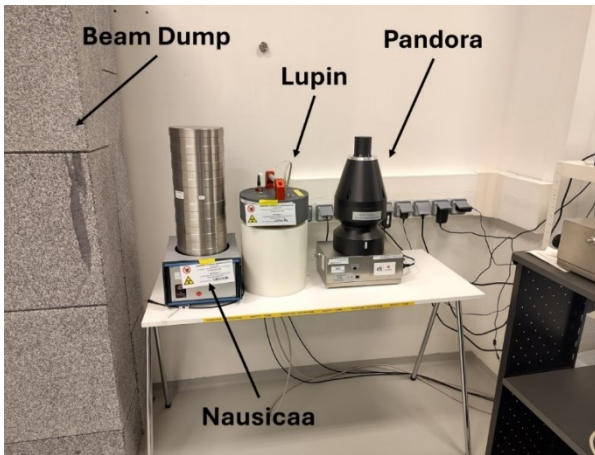


Figure 4: Setup of dosimeters for the measurement campaign in the ALFA experimental hall.

3.3. Monte Carlo Simulation

The Monte Carlo Simulation (MCS) has been carried out using the FLUKA code (version FLUKA4-4.0) and the FLAIR interface. The geometry of the laser building was already available and has been coded by the Monte Carlo Working Group in ELI Beamlines for radiation protection studies. This geometry has been complemented by details about the specific setup of the ALFA experimental line and the ALFA vacuum chamber. A view of the FLUKA geometry of the ALFA experimental hall coded for the MCS can be seen in **Figure 5**.

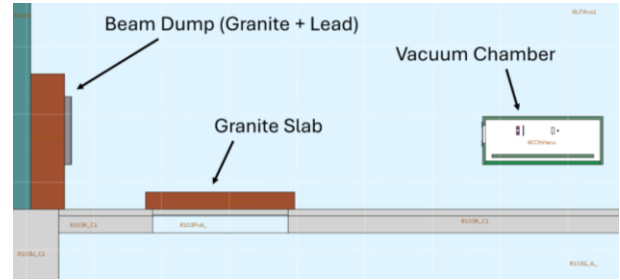


Figure 5: FLUKA geometry model of a portion of the ALFA experimental station, side view.

The source term has three components: the Quasi-Mono-Energetic (QME) electron beam; the low energy electron beam; the photon beam. The source characteristics have been coded through a source subroutine in FLUKA and the simulation has been ultimately run with 10^5 primaries. A plot of the source spectrum employed in the MCS can be seen in **Figure 6**.

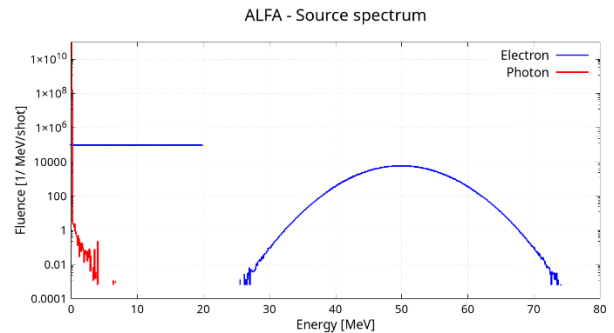


Figure 6: FLUKA plot illustrating the source term spectrum resulting from a simulation run with 10^5 primary particles. The red line indicates the photon beam, the uniform blue distribution on the left side corresponds to the low-energy background electron beam, and the Gaussian blue distribution represents the QME electron beam.

4. Results

4.1. Dataset

The dataset refers to the measurement campaign of 11-15 March 2024, encompassing a full week of irradiation experiments at ALFA. Considering that the Pandora dosimeter is equipped with two distinct and independent detection channels the following description will address gammas and neutrons separately. This approach will facilitate a more detailed analysis and a side-by-side comparison between the Lupin-Pandora (for neutrons) and Nausicaa-Pandora (for gamma particles) systems.

4.2. Neutrons

Figure 7 illustrates the dose-rates recorded by the Lupin dosimeter and the neutron component of the Pandora dosimeter during operations on March 13, 2024.

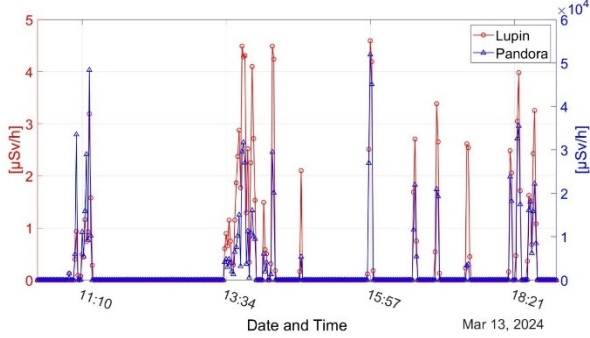


Figure 7: Plot of the dose-rates detected in the ALFA experimental hall by the Lupin dosimeter (represented by red circles) and the Pandora dosimeter (represented by blue triangles). Due to the differing orders of magnitude of the dose-rates recorded by the two dosimeters, the Lupin data is plotted against the left vertical axis, while the Pandora data is plotted against the right vertical axis.

The dose rates recorded by the two dosimeters are represented on distinctly different scales, necessitating the use of separate vertical axes for the two plots. Specifically, the peaks detected by the Lupin dosimeter reach $4.5 \mu\text{Sv/h}$, whereas those recorded by the Pandora exceed $5 \cdot 10^4 \mu\text{Sv/h}$, demonstrating a remarkable difference of four orders of magnitude. This pattern is consistently observed throughout the entire week.

However, a closer examination of the data from the Pandora indicated that this discrepancy was due to the high-energy neutron channel of the detector. An examination of the source spectrum plotted in **Figure 5** indicates that a low number of neutrons are expected to be produced with energies exceeding 20 MeV. Since secondary particles can be generated with energies equal to or lower than those of the primary particles that produced them, only high-energy electrons can indirectly contribute to this production. The most probable mechanism for neutron production in this context involves gamma rays generated by bremsstrahlung, inelastic scattering, and pair production. These gamma rays can subsequently produce neutrons via photonuclear reactions.

The assertion that the number of neutrons with energies above 20 MeV is low is supported by the fluence obtained from the Monte Carlo simulation carried out with the parameters

detailed in Paragraph 3.3. As shown in **Figure 8**, the results of the Monte Carlo simulation indicate that the majority of neutrons do not exceed 5 MeV. Although there are significant systematic uncertainties associated with the simulations, it is highly unlikely that a substantial number of neutrons have been produced at higher energies. Consequently, it is suggested that the dose-rates recorded in the high-energy neutron channel of the Pandora dosimeter may not be reliable in this context.

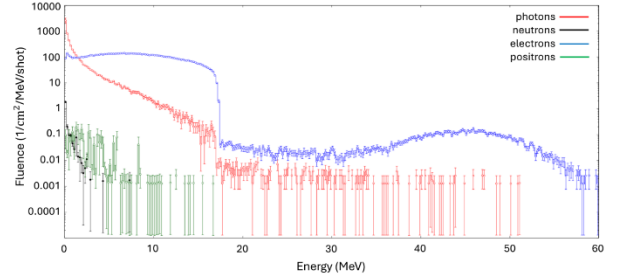


Figure 8: FLUKA plot illustrating the fluence across the mockup detector positioned close to the beam dump.

Consequently, the low-energy component of the Pandora detector was examined in comparison to the dose rate recorded by the Lupin detector. Since each dosimeter captures data from the electronics at slightly different frequencies, or the convolution of the ultra-short pulses may vary, a viable solution is to calculate the integral of each individual peak and compare it with the corresponding integral of the peaks recorded by the other detector. This integration is performed using an algorithm that automatically identifies the data samples associated with the same peak by detecting the minimum values among two consecutive peaks. Subsequently, the integral is calculated between two adjacent minima. This integration method helps to mitigate synchronization issues between the datasets.

The average ratio between the integrated doses of the two dosimeters is 3.4, meaning that the dose detected by the Lupin is, on average, three times higher than the dose detected by the Pandora. The level of difference that persists, even when considering only the low-energy neutron channel of the Pandora dosimeter, is considerably more acceptable and justifiable within the unique environment of a laser-driven accelerator.

Furthermore, the placement of the detectors may affect the fluence of particles incident upon each individual detector. Given that a portion of the neutrons is expected to be generated during interactions with the beam dump, it is plausible that a shielding effect of the Lupin on the

Pandora occurred (refer to Figure 4). Additionally, a higher underestimation of the Pandora dosimeter with respect to the Lupin when working in pulsed fields with high doses per burst is in accordance with the literature [3].

4.3. Gamma Particles

The discussion regarding the dose delivered by gamma particles is more straightforward, as no anomalies similar to those observed in the neutron measurements have been detected. However, some discrepancies between the Nausicaa dosimeter and the Pandora dosimeter are still present.

Figure 9 presents a histogram comparing the integrated peak values obtained for the Nausicaa dosimeter with those corresponding to the Pandora dosimeter, along with the peak-to-peak ratio between the two results. This evaluation follows the same process described for the neutrons case.

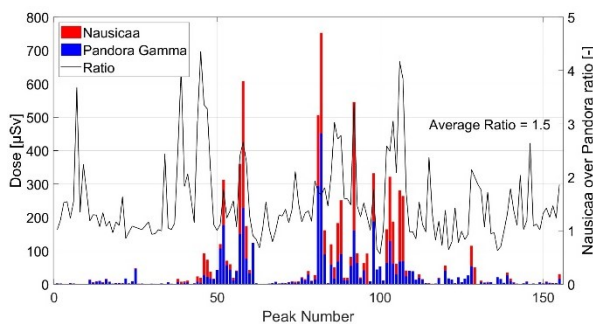


Figure 9: Histogram of the integral of each peak evaluated from the gamma particles dose-rate detected by the Nausicaa dosimeter (represented in red), compared with the corresponding peak integral detected by the Pandora dosimeter (represented in blue). The black curve illustrates the computed ratio between the integrated doses of the two dosimeters.

The findings indicate that the average ratio is 1.5, with Nausicaa consistently detecting higher doses in the majority of cases. As anticipated, none of the detectors utilized in this study are specifically designed to accurately measure dose rates as high as those encountered in the vicinity of the ALFA station. Consequently, a factor of 1.5 difference between the measurements from the two dosimeters is considered an acceptable outcome.

4.4. High Energy Neutrons

The high-energy neutron doses detected by the Pandora dosimeter appear to be not completely reliable in this context for the reasons outlined

above. However, it would be valuable to investigate the mechanisms underlying this behavior and to identify the specific dose-rates at which it can be observed. One potential explanation is that the ultra-short, high-intensity bursts of gamma radiation impacting the detector are being misidentified as high-energy neutrons. In support of this hypothesis, **Figure 10** illustrates a clear correlation between the dose rates of high-energy neutrons and gamma particles.

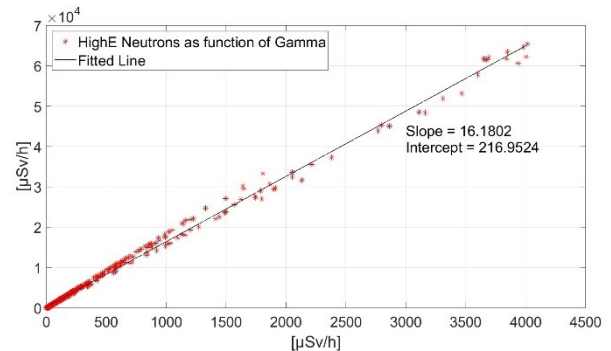


Figure 10: Plot of the dose-rate of the high-energy neutron component detected by the Pandora dosimeter as a function of the gamma particle dose-rate. The black line represents the linear regression of the scatter plot.

To further investigate the results of this analysis, an R-squared test was conducted, obtaining a value of 0.997, which indicates a very high correlation. In contrast, the analysis of the correlation between the high-energy and low-energy neutron components yields an R-squared value of 0.670. While this value is still relatively high, reflecting the simultaneous production of all types of radiation, it is notably lower compared to the correlation observed between high-energy neutrons and gamma particles. The correlation plot between high-energy and low-energy neutron components is shown in **Figure 11**.

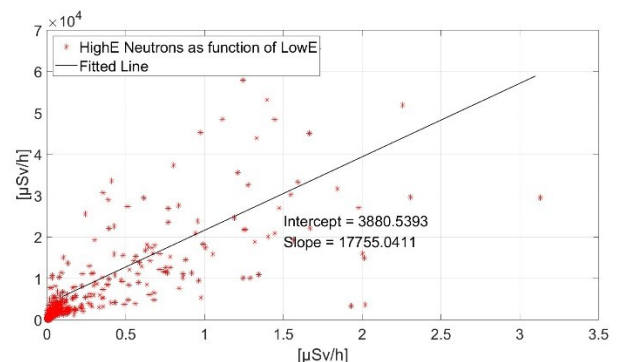


Figure 11: Plot of the dose-rate of the high-energy neutron component detected by the Pandora dosimeter as a function of the low-energy neutron dose-rate. The black line

represents the linear regression of the scatter plot.

Additional information can be obtained from the examination of the two supplementary Pandora dosimeters located in the vicinity of the experimental hall. One dosimeter was situated in the control room, several meters away from the beam, while the other was positioned in the west corridor, directly on the opposite side of the wall adjacent to the beam dump.

What emerges is that the Pandora positioned in the west corridor, where the radiation levels are two orders of magnitude lower than the levels present in the experimental hall, still exhibit anomalous behavior. This suggests that the misdetection is not attributable to a defective dosimeter, but rather to its inherent design.

In contrast, the plots for the Pandora positioned in the control room do not exhibit the same effect. In the high-energy neutron channel, only a stochastic signal is attributable to the background is recorded, while the other two channels continue to display radiation peaks at low dose-rate levels. Since very low dose-rate levels are expected in the control room, due to the distance and the angle from the direction of the beam, the results of the Pandora are supposed to be reliable in this context, suggesting that the misdetection of high-energy neutrons is a threshold phenomenon that occurs when the dosimeter is exposed to high dose-rate values.

Finally, a detailed examination of the irradiation campaign conducted between 17:00 and 19:30 on March 13, 2024, is presented. There has been six irradiations delivered in this timespan, with duration ranging from 60 to 120 s and estimated beam charges going from $5 \cdot 10^4 e^-$ to $11 \cdot 10^4 e^-$.

Irradiations #2 to #4 employ the same setup and irradiation duration, however, irradiation #4 incorporates a magnet specifically designed to divert the low-energy component of the radiation. Due to the neutrality of the neutron particle, it is expected that the three peaks corresponding to irradiations #2 to #4 will exhibit similar values in both the high-energy and low-energy neutron channels. It is also expected that the gamma particle peak associated with irradiation #4 will be lower than those of irradiations #2 and #3. This reduction is attributed to the decrease in bremsstrahlung radiation directed toward the dosimeters, resulting from the diversion of the charged particle component of the beam (i.e., electrons).

Figure 12 presents the dose-rate plots recorded by the Pandora dosimeter positioned near the

beam dump during the examined time period. Notably, the high-energy neutron and gamma particle channels exhibit identical radiation profiles, characterized by two peaks of approximately equal magnitude, with the latter peak being significantly smaller. In contrast, the low-energy neutron channel displays three similar peaks, consistent with the neutral nature of neutrons, which cannot be deflected by a magnetic field.

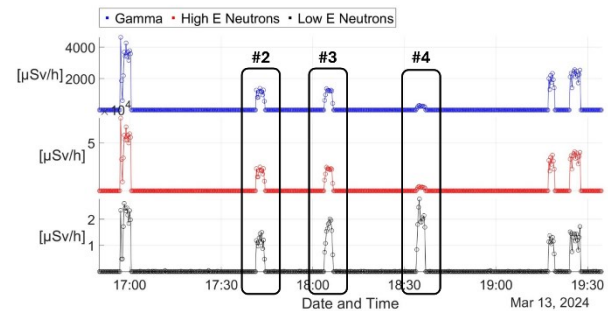


Figure 12: Plots of the dose-rates detected by a Pandora in the ALFA experimental hall on March 13, 2024, between 17:00 and 19:30. Each subplot refers to a single radiation component. From top to bottom: gamma particles, high-energy neutrons, low-energy neutrons.

For reference, **Figure 13** displays the dose rates recorded by the Lupin dosimeter under the same conditions. The plot of the radiation levels detected by the Lupin indicates that peaks #2, #3, and #4 are similar to one another, as expected.

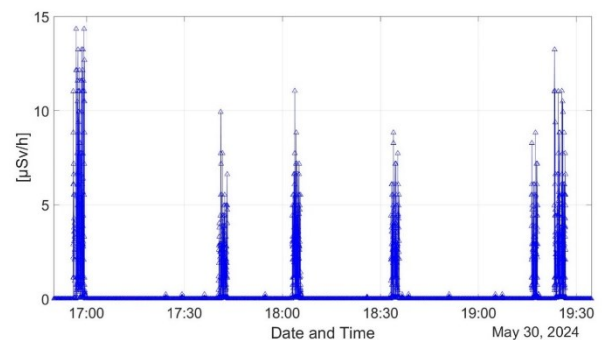


Figure 13: Plot of the dose-rates detected by a Lupin dosimeter in the ALFA experimental hall on March 13, 2024, between 17:00 and 19:30.

This finding further supports the hypothesis that the high-energy neutron channel of the Pandora dosimeter is influenced by gamma particle radiation. In this instance, the correlation is suggested by physical considerations rather than by numerical data analysis, as discussed previously. This reinforces the body of evidence and simultaneously reduces the likelihood of erroneous data manipulation.

5. Conclusions

The thesis employs a combination of dosimetric measurements and Monte Carlo simulations to analyze the secondary radiation produced during the acceleration process. The three dosimeters utilized in this study were tested under conditions characterized by high charge per bunch, short temporal duration, and a repetition frequency of 1 kHz, which present significant challenges for conventional radiation detection devices.

The analysis of the collected data revealed anomalous behavior by a detection channel of one of the dosimeters, which was considered to be unreliable due to technical and physical considerations. The results obtained from the other detectors were compared, providing a comprehensive overview of the detection levels in the vicinity of the ALFA station.

Furthermore, a detailed examination of the anomalous behavior of the Pandora dosimeter was conducted through data analysis and comparisons. This investigation highlighted the correlation between gamma particles and the high-energy neutron channels of the detector, suggesting that the observed behavior is attributable to the high charge per bunch impacting the dosimeters in ultra-short pulses.

The study underscores the necessity for further research to understand these phenomena, including controlled experiments and a thorough examination of the dosimeter's electronics.

6. References

- [1] Cimmino A. *et al.*, Nuclear Science and Engineering **198**, 245-263 (2024).
- [2] Lazzarini C.M. *et al.*, Phys. Plasmas **31**, 030703 (2024).
- [3] Caresana M. *et al.*, Rev. Sci. Instrum. **85**, 065102 (2014).